D^0 Mixing at Belle

L. M. Zhang (on behalf of the Belle Collaboration)
Syracuse University, Syracuse, New York 13244, USA

We report the recent two results of D^0-$\overline{D}^0$ mixing studies at Belle in $D^0 \to K^+K^-/\pi^+\pi^-$ and $D^0 \to K^0_S\pi^+\pi^-$ decays. The former measures the relative difference of the lifetimes y_{CP}, giving the evidence of D^0-$\overline{D}^0$ mixing; the latter measures the D^0 mixing parameters x and y.

1. Introduction

Mixing phenomenon, i.e. the oscillation of a neutral meson into its corresponding anti-meson as a function of time, has been observed in the K^0, B^0, and most recently B^0_s systems. This process is also possible in the D-meson system, but has not previously been observed.

Mixing in heavy flavor systems such as that of B^0 and B^0_s is governed by the short-distance box diagram. However, in the D^0 system this diagram is both GIM-suppressed and doubly-Cabibbo-suppressed relative to the amplitude dominating the decay width, and thus the short-distance rate is very small. Consequently, D^0-$\overline{D}^0$ mixing is expected to be dominated by long-distance processes that are difficult to calculate; theoretical estimates for the mixing parameters $x = (m_1 - m_2)/\Gamma$ and $y = (\Gamma_1 - \Gamma_2)/2\Gamma$ range over two-three orders of magnitude [1]. Here, m_1, m_2 (Γ_1, Γ_2) are the masses (decay widths) of the mass eigenstates $|D_{1,2}\rangle = p|D^0\rangle \pm q|\overline{D}^0\rangle$, and $\Gamma = (\Gamma_1 + \Gamma_2)/2$. The parameters p and q are complex coefficients satisfying $|p|^2 + |q|^2 = 1$.

The general experimental method identifies the flavor of the neutral D meson when produced by reconstructing the decay $D^{*+} \to D^0\pi^+$ or $D^{*-} \to \overline{D}^0\pi^-$ [2]; the charge of the accompanying pion identifies the D flavor. Because the energy release in D^* decays is only ~ 6 MeV, the background is largely suppressed. The D^0 decay time (t) is calculated via $(l/p) \times m_{D^0}$, where l is the distance between the D^* and D^0 decay vertices and p is the D^0 momentum. The D^* vertex position is taken to be the intersection of the D^0 momentum with the beamspot profile. To reject $D^{(*)}$ decays originating from B decays, one requires $p_{D^*} > 2.5$ GeV, which is the kinematic endpoint.

2. CP-eigenstates K^+K^- and $\pi^+\pi^-$

We have studied the decays to CP eigenstates $D^0 \to K^+K^-$and $D^0 \to \pi^+\pi^-$; treating the decay-time distributions as exponential, we measured the quantity

$$y_{CP} = \frac{\tau_{K^-\pi^+}}{\tau_{K^+K^-}} - 1, \qquad (1)$$

where $\tau_{K^-\pi^+}$ and $\tau_{K^+K^-}$ are the lifetimes of $D^0 \to K^-\pi^+$ and $D^0 \to K^+K^-$(or $D^0 \to \pi^+\pi^-$) decays. It can be shown that $y_{CP} = y\cos\phi - \frac{1}{2}A_M x \sin\phi$ [3], where A_M parameterizes CPV in mixing and ϕ is a weak phase. If CP is conserved, $A_M = \phi = 0$ and $y_{CP} = y$. This method has been used by numerous experiments to constrain $y_{\rm CP}$ [4]. Our measurement, based on 540 fb^{-1} data, yields a nonzero value of y_{CP} with $> 3\sigma$ significance [5]. We also searched for CPV by measuring the quantity

$$A_\Gamma = \frac{\tau(\overline{D}^0 \to K^-K^+) - \tau(D^0 \to K^+K^-)}{\tau(\overline{D}^0 \to K^-K^+) + \tau(D^0 \to K^+K^-)}; \qquad (2)$$

this observable equals $A_\Gamma = \frac{1}{2}A_M y\cos\phi - x\sin\phi$ [3].

We reconstruct $D^{*+} \to D^0\pi^+_s$ decays and $D^0 \to K^+K^-$, $K^-\pi^+$, and $\pi^+\pi^-$. Candidate D^0 mesons are selected using two kinematic observables: the invariant mass of the D^0 decay products, M, and the energy release in the D^{*+} decay, $Q = (M_{D^*} - M - m_{\pi^+})c^2$. According to Monte Carlo (MC) simulated distributions of t, M and Q, background events fall into four categories: (1) combinatorial, with zero apparent lifetime; (2) true D^0 mesons combined with random slow pions (this has the same apparent lifetime as the signal) (3) D^0 decays to three or more particles, and (4) other charm hadron decays. The apparent lifetime of the latter two categories is 10-30% larger than τ_{D^0}.

For the lifetime measurements, we select the events satisfying $|\Delta M|/\sigma_M < 2.3$, $|Q - 5.9$ MeV$| < 0.80$ MeV and $\sigma_t < 370$ fs, where $\Delta M \equiv M - m_{D^0}$, and σ_t is the decay time uncertainties calculated event-by-event. The invariant mass resolution σ_M varies from 5.5-6.8 MeV/c^2, depending on the decay channel. The selection criteria are chosen to minimize the expected statistical error on y_{CP} using the MC. We find 111×10^3 K^+K^-, 1.22×10^6 $K^-\pi^+$ and 49×10^3 $\pi^+\pi^-$ signal events, with purities of 98%, 99% and 92% respectively.

The relative lifetime difference y_{CP} is determined by performing a simultaneous binned maximum likelihood fit to the $D^0 \to K^+K^-$, $D^0 \to K^+\pi^-$, $D^0 \to \pi^+\pi^-$decay time distributions. Each distribution is assumed to be a sum of signal and background contributions, with the signal contribution being a convolution of an exponential and a detector resolution

function,

$$dN/dt = \frac{N_{\rm sig}}{\tau} \int e^{-t'}\tau \cdot R(t-t')\,dt' + B(t). \quad (3)$$

The resolution function $R(t-t')$ is constructed from the normalized distribution of the decay time uncertainties σ_t. The σ_t of a reconstructed event ideally represents an uncertainty with a Gaussian probability density: in this case, bin i in the σ_t distribution is taken to correspond to a Gaussian resolution term of width σ_i, with a weight given by the fraction f_i of events in that bin. However, the distribution of "pulls", i.e. the normalized residuals $(t_{\rm rec} - t_{\rm gen})/\sigma_t$ (where $t_{\rm rec}$ and $t_{\rm gen}$ are reconstructed and generated decay times), is not well-described by a Gaussian. We found that this distribution can be fitted with a sum of three Gaussians of different widths $\sigma_k^{\rm pull}$ and fractions w_k, constrained to the same mean. Therefore, we choose the parameterization

$$R(t-t') = \sum_{i=1}^{n} f_i \sum_{i=1}^{3} w_k G(t-t';\sigma_{ik},t_0), \quad (4)$$

with $\sigma_{ik} = s_k \sigma_k^{\rm pull} \sigma_i$, where the s_k are three scale factors introduced to account for differences between the simulated and real $\sigma_k^{\rm pull}$, and t_0 allows for a (common) offset of the Gaussian terms from zero.

The background $B(t)$ is parameterized assuming two lifetime components: an exponential and a δ function, each convolved with corresponding resolution functions as parameterized by Eq. (4). Separate $B(t)$ parameters for each final state are determined by fits to the t distributions of events in M sidebands. The MC is used to select the sideband region that best reproduces the timing distribution of background events in the signal region.

Fitting the $K^-\pi^+$, K^+K^-, and $\pi^+\pi^-$ decay time distributions (Figs. 1(a)-(c)) shows a statistically significant difference between the $K^-\pi^+$ and h^+h^- lifetimes. The effect is visible in Fig. 1d, which plots the ratio of event yields $N_{h^+h^-}/N_{K\pi}$ as a function of decay time. The fitted lifetime of D^0 meson in the $K^-\pi^+$ final states is 408.7 $\pm$ 0.6 fs, which is consistent with the PDG value [6] (and actually has greater statistical precision). We measure

$$y_{\rm CP} \;=\; (1.31 \pm 0.32 \pm 0.25)\%\,, \quad (5)$$

which deviates from zero by 3.2σ. The systematic error is dominated by uncertainty in the background decay time distribution, variation of selection criteria, and the assumption that t_0 is equal for all three final states. The analysis also measures

$$A_\Gamma \;=\; (0.01 \pm 0.30 \pm 0.15)\%\,, \quad (6)$$

which is consistent with zero (no CPV). The sources of systematic error for A_Γ are similar to those for $y_{\rm CP}$.

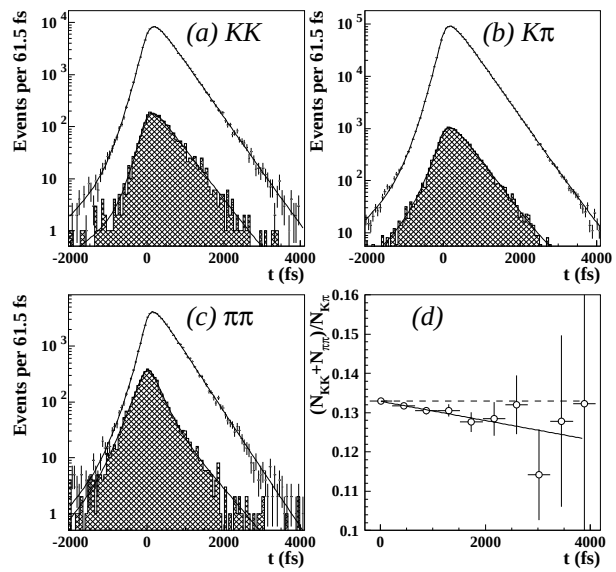

Figure 1: Projections of the decay-time fit superimposed on the data for $D^0 \to K^+K^-$, $D^0 \to K^-\pi^+$, and $D^0 \to \pi^+\pi^-$ decays. The hatched area represents the background contribution. Plot *(d)* shows the ratio of decay-time distributions for $D^0 \to (K^+K^- + \pi^+\pi^-)$ and $D^0 \to K^-\pi^+$; the solid line is a fit to the points.

3. Dalitz Plot Analysis of $D^0 \to K_S^0\,\pi^+\pi^-$

The time dependence of the Dalitz plot for $D^0 \to K_S^0\,\pi^+\pi^-$ decays is sensitive to mixing parameters x and y without ambiguity due to strong phases. For a particular point in the Dalitz plot (m_+^2, m_-^2), where $m_+ \equiv m(K_S^0\,\pi^+)$ and $m_- \equiv m(K_S^0\,\pi^-)$, the overall decay amplitude is

$$\mathcal{A}_{D^0}(m_+^2,m_-^2)\,\frac{e_1(t)+e_2(t)}{2} \;+\; \left(\frac{q}{p}\right)\mathcal{A}_{\overline{D}^0}(m_+^2,m_-^2)\,\frac{e_1(t)-e_2(t)}{2}\,, \quad (7)$$

where $e_{(1,2)}(t) = e^{-(im_{1,2}+\Gamma_{1,2}/2)t}$. The first term represents the (time-dependent) amplitude for $D^0 \to K_S^0\,\pi^+\pi^-$, and the second term represents the amplitude for $D^0 \to \overline{D}^0 \to K_S^0\,\pi^+\pi^-$. Taking the modulus squared of Eq. (7) gives the decay rate or, equivalently, the density of points $\rho(m_+^2, m_-^2; t)$. The result contains terms proportional to $\cosh(y\,\Gamma t)$, $\cos(x\,\Gamma t)$, and $\sin(x\,\Gamma t)$, and thus fitting the time-dependence of $\rho(m_+^2, m_-^2; t)$ determines x and y. This method was developed by CLEO [7].

To use Eq. (7) requires choosing a model for the decay amplitudes $\mathcal{A}_{D^0,\overline{D}^0}(m_+^2, m_-^2)$. This is usually taken to be the "isobar model" [8], and thus, in addition to x and y, one also fits for the magnitudes and phases of various intermediate states. Specifically, $\mathcal{A}_{D^0}(m_+^2, m_-^2) = \sum_j a_j\, e^{i\delta_j}\, A_j$, where δ_j is a

strong phase, A_j is the product of a relativistic Breit-Wigner function and Blatt-Weiskopf form factors, and the parameter j runs over all intermediate states. This sum includes possible scalar resonances and, typically, a constant non-resonant term. For no direct CPV, $\mathcal{A}_{\overline{D}^0}(m_+^2, m_-^2) = \mathcal{A}_{D^0}(m_-^2, m_+^2)$; otherwise, one must consider separate decay parameters (a_j, δ_j) for D^0 decays and $(\bar{a}_j, \bar{\delta}_j)$ for $\overline{D}^0$ decays.

We have fit a large $D^0 \to K_S^0\,\pi^+\pi^-$ sample selected from 540 fb^{-1} of data [9]. The analysis proceeds in two steps. First, signal and background yields are determined from a two-dimensional fit to variables $M(K\pi\pi)$ and $Q = M(\pi_s K\pi\pi) - M(K\pi\pi) - m_{\pi^+}$. Within a signal region $|M(K\pi\pi) - m_{D^0}| < 15$ MeV/c^2 and $|Q - 5.9$ MeV$| < 1.0$ MeV (corresponding to 3σ in resolution), there are 534 000 signal candidates with 95% purity. These events are fit for x and y; the (unbinned ML) fit variables are m_+^2, m_-^2, and the decay time t. Most of the background is combinatoric, i.e., the D^0 candidate results from a random combination of tracks. The decay-time distribution of this background is modeled as the sum of a delta function and an exponential function convolved with a Gaussian resolution function, and all parameters are determined from fitting events in the sideband 30 MeV/$c^2 < |M(K\pi\pi) - m_{D^0}| < 55$ MeV/c^2.

The results from two separate fits are listed in Table I. In the first fit CP conservation is assumed, i.e., $q/p = 1$ and $\mathcal{A}_{\overline{D}^0}(m_+^2, m_-^2) = \mathcal{A}_{D^0}(m_-^2, m_+^2)$. The free parameters are x, y, τ_{D^0}, some timing resolution function parameters, and decay model parameters (a_r, δ_r). The results for the latter are listed in Table II. The results for x and y indicate that x is positive, about 2σ from zero. Projections of the fit are shown in Fig. 2. The fit also yields $\tau_D = (409.9 \pm 1.0)$ fs, which is consistent with the PDG value [6] (and actually has greater statistical precision).

Table I Fit results and 95% C.L. intervals for x and y, from analysis of $D^0 \to K_S^0\,\pi^+\pi^-$ decays. The errors are statistical, experimental systematic, and decay-model systematic, respectively.

Fit	Param.	Result	95% C.L. inter.
No	x (%)	$0.80 \pm 0.29\,^{+0.09}_{-0.07}\,^{+0.10}_{-0.14}$	$(0.0, 1.6)$
CPV	y (%)	$0.33 \pm 0.24\,^{+0.08}_{-0.12}\,^{+0.06}_{-0.08}$	$(-0.34, 0.96)$
CPV	x (%)	$0.81 \pm 0.30\,^{+0.10}_{-0.07}\,^{+0.09}_{-0.16}$	$\lvert x\rvert < 1.6$
	y (%)	$0.37 \pm 0.25\,^{+0.07}_{-0.13}\,^{+0.07}_{-0.08}$	$\lvert y\rvert < 1.04$
	$\lvert q/p\rvert$	$0.86\,^{+0.30}_{-0.29}\,^{+0.06}_{-0.03} \pm 0.08$	–
	ϕ (°)	$-14\,^{+16}_{-18}\,^{+5}_{-3}\,^{+2}_{-4}$	–

For the second fit, CPV is allowed and the D^0 and $\overline{D}^0$ samples are considered separately. This introduces additional parameters $|q/p|$, $\mathrm{Arg}(q/p) = \phi$, and $(\bar{a}_j, \bar{\delta}_j)$. The fit gives two equivalent solutions, (x, y, ϕ) and $(-x, -y, \phi + \pi)$. Aside from this pos-

Table II Fit results for $D^0 \to K_S^0\,\pi^+\pi^-$ Dalitz plot parameters. The errors are statistical only. The fit fraction is defined as the ratio of the integral $\int |a_r\,\mathcal{A}_r(m_-^2, m_+^2)|^2\,dm_-^2\,dm_+^2$ to $\int |\sum_{r=1}^n a_r\,e^{i\delta_r}\,\mathcal{A}_r(m_-^2, m_+^2)|^2\,dm_-^2\,dm_+^2$.

Resonance	Amplitude	Phase (deg)	Fit fraction
$K^*(892)^-$	1.629 ± 0.006	134.3 ± 0.3	0.6227
$K_0^*(1430)^-$	2.12 ± 0.02	-0.9 ± 0.8	0.0724
$K_2^*(1430)^-$	0.87 ± 0.02	-47.3 ± 1.2	0.0133
$K^*(1410)^-$	0.65 ± 0.03	111 ± 4	0.0048
$K^*(1680)^-$	0.60 ± 0.25	147 ± 29	0.0002
$K^*(892)^+$	0.152 ± 0.003	-37.5 ± 1.3	0.0054
$K_0^*(1430)^+$	0.541 ± 0.019	91.8 ± 2.1	0.0047
$K_2^*(1430)^+$	0.276 ± 0.013	-106 ± 3	0.0013
$K^*(1410)^+$	0.33 ± 0.02	-102 ± 4	0.0013
$K^*(1680)^+$	0.73 ± 0.16	103 ± 11	0.0004
$\rho(770)$	1 (fixed)	0 (fixed)	0.2111
$\omega(782)$	0.0380 ± 0.0007	115.1 ± 1.1	0.0063
$f_0(980)$	0.380 ± 0.004	-147.1 ± 1.1	0.0452
$f_0(1370)$	1.46 ± 0.05	98.6 ± 1.8	0.0162
$f_2(1270)$	1.43 ± 0.02	-13.6 ± 1.2	0.0180
$\rho(1450)$	0.72 ± 0.04	41 ± 7	0.0024
σ_1	1.39 ± 0.02	-146.6 ± 0.9	0.0914
σ_2	0.267 ± 0.013	-157 ± 3	0.0088
NR	2.36 ± 0.07	155 ± 2	0.0615

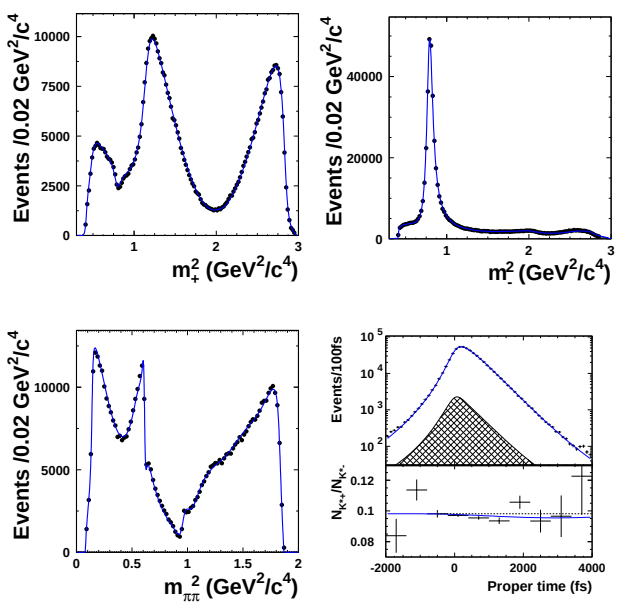

Figure 2: Projection of the unbinned ML fit superimposed on the data for $D^0 \to K_S^0\,\pi^+\pi^-$ decays. In *(d)*, the hatched area represents the combinatorial background contribution, and the lower plot shows the ratio of decay-time distributions for events in the $K^*(892)^+$ and $K^*(892)^-$ regions, where sensitivity to (x, y) is highest.

sible sign change, the effect upon x and y is small, and the results for $|q/p|$ and ϕ are consistent with no CPV. The sets of Dalitz parameters (a_r, δ_r) and $(\bar{a}_r, \bar{\delta}_r)$ are consistent with each other, indicating no direct CPV. Taking $a_j = \bar{a}_j$ and $\delta_j = \bar{\delta}_j$ (i.e., no direct CPV) and repeating the fit gives $|q/p| = 0.95\,^{+0.22}_{-0.20}$ and $\phi = (-2\,^{+10}_{-11})^\circ$.

The dominant systematic errors are from the time dependence of the Dalitz plot background, and the effect of the p_{D^*} momentum cut used to reject D^*'s originating from B decays. The default fit includes $\pi\pi$ scalar resonances σ_1 and σ_2; when evaluating systematic errors, the fit is repeated without any $\pi\pi$ scalar resonances using K-matrix formalism [10]. The influence upon x and y is small and included as a systematic error.

The 95% C.L. contour for (x, y) is plotted in Fig. 3. The contour is obtained from the locus of points where $-2\ln\mathcal{L}$ rises by 5.99 units from the minimum value; the distance of the points from the origin is subsequently rescaled to include systematic uncertainty. We note that for the CPV-allowed case, the reflections of the contours through the origin are also allowed regions.

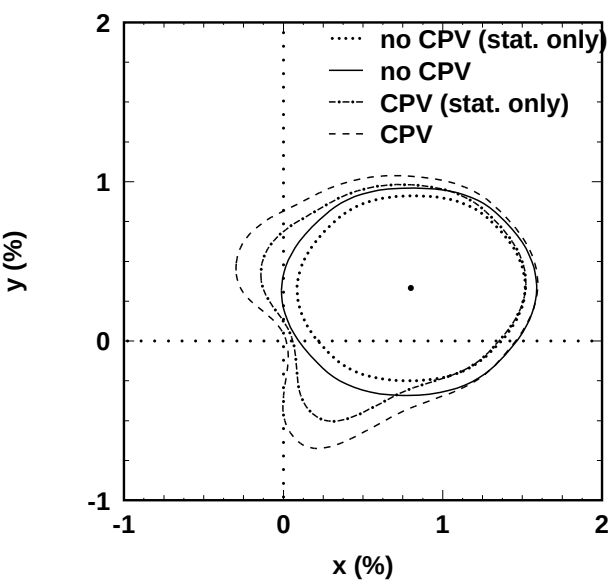

Figure 3: 95% C.L. contours for (x, y): dotted (solid) is statistical (statistical plus systematic) contour for no CPV; dashed-dotted (dashed) is statistical (statistical plus systematic) contour allowing for CPV. The point is the best-fit value for no CPV.

References

[1] A. A. Petrov, Int. J. Mod. Phys. A**21**, 5686 (2006); arXiv:hep-ph/0611361.

[2] Charge-conjugate modes are included unless noted otherwise.

[3] S. Bergmann *et al.*, Phys. Lett. B **486**, 418 (2000).

[4] E. M. Aitala *et al.* (E791), Phys. Rev. Lett. **83**, 32 (1999); J. M. Link *et al.* (FOCUS), Phys. Lett. B **485**, 62 (2000); S. E. Csorna *et al.* (CLEO), Phys. Rev. D **65**, 092001 (2002); B. Aubert *et al.* (*BABAR*), Phys. Rev. Lett. **91**, 121801 (2003).

[5] M. Staric *et al.* (Belle), Phys. Rev. Lett. **98**, 211803 (2007).

[6] W.-M. Yao *et al.* (PDG), Jour. of Phys. G **33**, 1 (2006).

[7] D. M. Asner *et al.* (CLEO), Phys. Rev. D **72**, 012001 (2005); arXiv:hep-ex/0503045 (revised April, 2007).

[8] A. Poluektov *et al.* (Belle), Phys. Rev. D **73**, 112009 (2006); S. Kopp *et al.* (CLEO), Phys. Rev. D **63**, 092001 (2001).

[9] L. M. Zhang *et al.* (Belle), Phys. Rev. Lett. **99**, 131803 (2007).

[10] J. M. Link *et al.* (FOCUS), Phys. Lett. B **585**, 200 (2004); B. Aubert *et al.* (*BABAR*), arXiv:hep-ex/0507101 (2005).